An X-ray Interferometer with a Large and Variable Path Length Difference

Many types of interferometers have been built and tested for x-ray applications. We present a Michelson-type instrument, which has the unique advantage of a large and variable path length difference. This first interferometer in its class has shown excellent fringe visibility in agreement with calculations.

In optical interferometry, the Michelson interferometer stands as one of the most important instruments. Two significant aspects of this interferometer are: (1) the path length difference (PLD) between the two interfering beams can be varied continuously and by any desired amount, and (2) the two beams have complete spatial overlap regardless of their PLD. This allows the interferometer to measure the temporal (or equivalently, the spectral) properties of the incoming electromagnetic radiation. The principle behind the Michelson interferometer is used in numerous instruments, including many modern-day telescopes and most Fourier transform spectrometers. It is therefore of interest to pursue an x-ray analogue to the Michelson interferometer. There have been several proposals for the x-ray equivalent of the Michelson's optical interferometer [1,2], but, until recently, none have been realized.

In the x-ray regime, beam manipulation is severely restricted because Bragg and/or Laue reflections have to be used to split and recombine the beam. X-ray mirrors can be used in special situations, but their utility is limited by their small (mrad) reflection angles. The first x-ray interferometer was the triple-Laue interferometer pioneered by Bonse and Hart [3]. X-ray interferometers have been used for phase-contrast imaging [4,5], measurement of atomic scattering factor dispersion corrections [6,7], high-precision metrology and distance calibration [8,9], the determination of the Avogadro number [10], and the measurement of beam coherence [11,12].

Appel and Bonse [13] first reported an x-ray interferometer with a variable PLD. This was the first true x-ray analogue of the Michelson optical interferometer. The small PLD, ~1 μm, however, limited its use. Izumi et al. [12] have reported on a wavefront-dividing x-ray interferometer with a *fixed* large (2.4 mm) PLD. By nature of its wavefront-division, however, the interfering beams suffer from a large 2 mm lateral shift (LS); i.e., the interfering beams do not overlap completely in space, and only the parts of the beam that do overlap interfere. It is thus not an x-ray analogue of the Michelson optical interferometer.

In this paper, an x-ray analogue of the Michelson optical interferometer, based on a variation of the all-Bragg Graeff-Bonse x-ray interferometer [14,15], is reported. This amplitude-division x-ray interferometer incorporates a *large* (~1 mm) *variable* PLD in the two interfering beams.

The interferometer uses complementary asymmetric Si(440) and Si(404) atomic planes in Bragg geometry. The beam is split into two coherent parts at the first reflecting surface (splitter) and recombined at the last reflecting surface (analyzer) after two additional Bragg reflections (mirrors). The fundamental energy for this interferometer is 7.46 keV for the Si(440)/Si(404) reflections. It is an amplitude-dividing interferometer, and, in theory, spatial beam coherence is *not* required for operation. This is fundamentally different from the wavefront-dividing interferometers. The approximate full-width half-maximum (FWHM) angular acceptance (Darwin width)

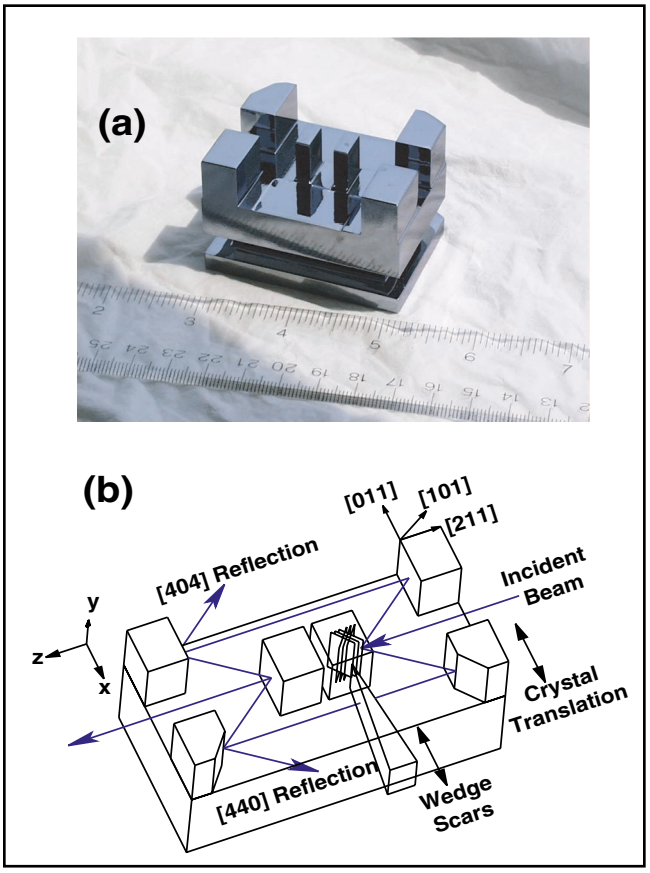

FIG. 1. Picture (a) and schematic (b) of the present variation of the Graeff-Bonse interferometer. The beam position shown is for x = 0, i.e., at the edge between the flat and the 1° slope part of the mirrors. The diffracting planes are sketched in the first reflecting surface (splitter).

and energy widths of the beam transmitted through the interferometer are, respectively, $\omega_D = 5$ [0.4] μrad and $\Delta E = 22$ [3.4] meV at 7.46 [14.92] keV.

In order to incorporate a large variable PLD between the two beams, a small angle (1°) was partly cut into the mirror (middle two reflections) faces in one of the arms of the interferometer (Fig. 1). The PLD thus varies depending on the incident beam location on the beam-splitter surface. In the experiment, varying the PLD involves translating the interferometer in the direction lateral to the incident beam. The small 1° additional cut causes very small angular changes in the beam directions (~1 μrad) that result in a small horizontal lateral shift or defocus at the analyzer surface on the order of 70 nm for the 7.46 keV-Si(440)/Si(404) case. For the 14.92 keV-Si(880)/Si(808) case, the LS is about four times smaller. Since the horizontal coherence length of the transmitted beam is expected to be in the 10 [100] μm range for the 7.46 [14.92] keV case, this small intrinsic shift can be neglected and will have no effect on the fringe visibility.

If the crystal was perfectly fabricated and the mirror symmetry perpendicular to the optical axis was preserved, there would be negligible LS everywhere (i.e., almost perfect overlap of the two partial beams at the exit surface), zero PLD on the flat part of the surfaces, and a linearly varying (depending on the beam location) PLD on the angled parts. Thus, in this respect, this interferometer is an x-ray analogue of the Michelson interferometer. In this design, a very large PLD (millimeters) is easily achievable and is limited only by the size of the silicon crystal. A larger angular cut in the mirror surfaces will also increase the achievable PLD.

Due to the limited accuracy of the fabrication and etching process, however, perfect symmetry of the crystal was not achieved. The crystal surfaces were measured using a high-resolution sapphire probe profilometer. Based on these measurements, the PLD and the LS of the two beam paths for each entrance point on the splitter surface were calculated (Fig. 2). Points for x > 0 denote the case in which the beam is on the flat part of the mirror(s), while x < 0

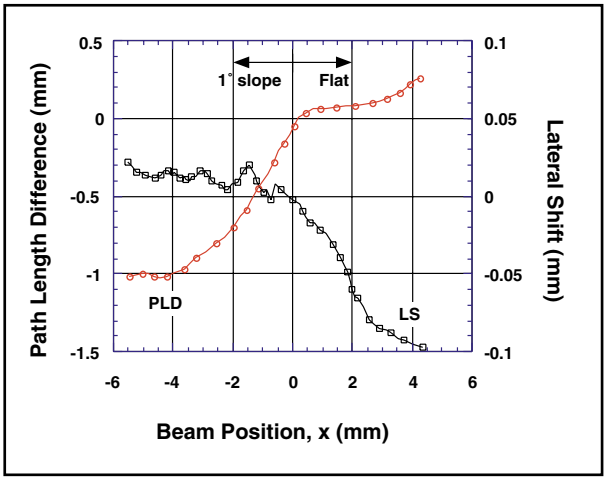

FIG. 2. The path length difference (PLD) and lateral shift (LS) of the crystal as a function of the beam position, calculated based on measurements done with a profilometer. x > 0 is the case in which the beam is on the flat part of the mirrors, and x < 0 is the case in which the beam is on the 1° slope part of the mirrors. While the variations in PLD were intended, the variations in LS were not (see text).

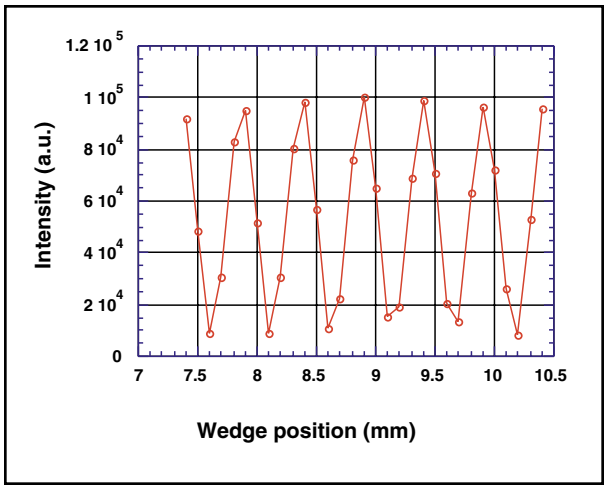

FIG. 3. A typical wedge scan at 7.46 keV and x = 0 mm.

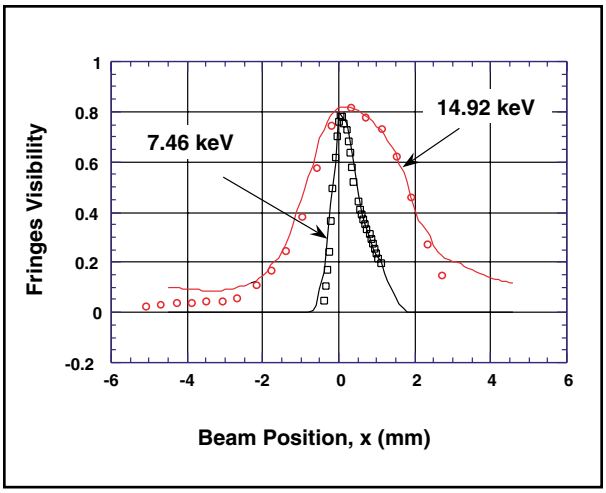

FIG. 4. Measured interference fringe visibility plotted as a function of the beam position x. The squares [circles] are the data points for 7.46 [14.92] keV, while the lines are from the fringe visibility analysis based on the crystal measurements in Fig. 2.

denotes the case in which the beam is on the part of the mirror (on one arm of the interferometer) where a 1° slope was cut.

The measurements were done on the SRI-CAT 1-ID beamline at the Advanced Photon Source (APS). An Si(111) double-crystal monochromator, which diffracts vertically, was upstream of the interferometer. The interferometer itself, 60 m away from the source, diffracted in the horizontal (electron orbit) plane. The APS undulator A source characteristics at 8 keV are σ_x = 359 μm [σ_y = 21 μm] for the horizontal [vertical] size and $\sigma_{x'}$ = 24 μrad [$\sigma_{y'}$ = 6.9 μrad] for the divergence. The slit sizes before the detector were set at 25 μm × 25 μm.

The experiment consisted of measuring the interference fringe visibility as a function of the PLD. Inserting a Plexiglas wedge in one path and translating it in the thickness gradient direction generates the fringes. A flat (and stationary) piece of Plexiglas was inserted into the other path to compensate for the average absorption loss due to the wedge. For a 4° wedge, a 0.5 mm wedge translation is equivalent to a 2π phase shift between the two beams at 7.46 keV (and 4π at 14.92 keV). A typical wedge scan at 7.46 keV is shown in Fig. 3. A wedge scan was done for each position of the beam on the crystal, and the resulting fringe contrast $(I_{max}-I_{min})/(I_{max}+I_{min})$ was plotted as a function of these positions. The data for the two energies are shown in Fig. 4. The squares (7.46 keV) and the circles (14.92 keV) are the data, and the lines are the computer simulations based on the measured PLD and LS for each beam position on the crystal.

The data analysis gives a longitudinal coherence length λ_L = 25 [175] μm and a horizontal transverse coherence length λ_T = 30 [200] μm at 7.46 [14.92] keV. These values are within 10% of expectations, based on the transmission spectrum and angular acceptance of the interferometer. Ideally, this interferometer would have negligible LS, and the fringe visibility would depend only on the longitudinal beam coherence. However, due to fabrication imperfections (Fig. 3), both longitudinal (λ_L) and transverse (λ_T) coherence lengths were involved.

In conclusion, the first x-ray interferometer with a large *and* variable path length difference has been constructed and successfully tested. Fringe visibility measurements agree with calculations.

The U.S. Department of Energy, Office of Science, Office of Basic Energy Sciences, under Contract No. W-31-109-ENG-38, supported this work.

Principal publication: "An X-ray Interferometer with a Large and Variable Path Length Difference," J. Appl. Cryst. **34**, 166-171 (2001).

References

[1] R. Deslattes, App. Phys. Lett. **12**, 133-135 (1968).

[2] M. Hart, Proc. R. Soc. Lond. A. **346**, 1-22 (1975).

[3] U. Bonse and M. Hart, App. Phys. Lett. **6**, 155-156 (1965).

[4] M. Ando and S. Hosoya, *Proc. 6th International Conference of X-ray Optics and Microanalysis*, edited by G. Shinoda, K. Kohra, and T. Ichinotawa (University of Tokyo Press, 1972).

[5] A. Momose, Nucl. Instrum. Methods, A**352**, 622-628 (1995).

[6] C. Cusatis and M. Hart, Proc. R. Soc. Lond. A**354**, 291-302 (1977).

[7] R. Begum, M. Hart, K.R. Lea, and D.P. Siddons, Acta Cryst. A**42**, 456-464 (1986).

[8] M. Hart, Brit. J. Appl. Phys. (J. Phys. D) **1**, 1405-1408.

[9] D.G. Chetwynd, S.C. Cockerton, S.T Smith, and W.W. Fung, Nanotechnology **2**, 1-10 (1991).

[10] R.D. Deslattes, A. Henins, H.A. Bowman, R.M. Schoonover, C.L. Carroll, I.L. Barnes, L.A. Machlan, L.J. Moore, and W.R. Shields, Phys. Rev. Lett. **33**, 463-466 (1974).

[11] H. Yamazaki and T. Ishikawa, SPIE Proceedings 2856, 279-288 (1996).

[12] K. Izumi, T. Mitsui, M. Seto, Y. Yoda, T. Ishikawa, X.W. Zhang, M. Ando, and S. Kikuta, Jpn. J. Appl. Phys. **34**, 5862-5868 (1995).

[13] A. Appel and U. Bonse, Phys. Rev. Lett. **67**, 1673-1676 (1991).

[14] W. Graeff and U. Bonse, Z. Physik B**27**, 19-32 (1977).

[15] K. Fezzaa and W.K. Lee, *Proc. SRI Eleventh US National Conference* (1999) pp. 167-173.

K. Fezzaa and W-K. Lee

User Program Division, Advanced Photon Source, Argonne National Laboratory, Argonne, IL, U.S.A.